ONE-DIMENSIONAL ROUTING OF MUD/DEBRIS FLOWS USING NWS FLDWAV MODEL

Ming Jin[1] and D. L. Fread[2]

ABSTRACT

A one-dimensional unsteady mud/debris flow modeling technique is being incorporated into the National Weather Service (NWS) FLDWAV dynamic flood routing model enhancing its capability to model unsteady flows of non-Newtonian fluids. This technique involves determining the friction slope of mud/debris flows based on a semi-empirical rheological power-law equation and a wave-front tracking technique. Three similar techniques are compared for model performance on three real-case mud/debris flow simulations and with some model sensitivity studies.

INTRODUCTION

Mud/debris floods, such as those caused by a landslide-induced mud/debris flow or those emanating from the dam-break-failure of a tailings or a debris dam, are a unique unsteady flow phenomenon in which the flow changes rapidly and the properties of moving fluid from the mixture of mud/debris and water are very different from pure water. One method of modeling this special flow is to use the one-dimensional dynamic unsteady flow equations by adding an additional friction slope term in the momentum equation according to the rheological properties of flowing mud/debris-water mixtures. The derivation of the friction slope term of the mud/debris flow depends on which rheological model (constitutive equation) for shear stress of a non-Newtonian fluid is used.

The NWS FLDWAV model is a generalized dynamic flood routing model based on an implicit weighted four-point, nonlinear, finite-difference solution of the

---

[1]Visiting Scientist, Hydrologic Research Laboratory, Office of Hydrology (Phone: 301-713-0640; Fax:301-713-0963; e-mail: ming.jin@noaa.gov

[2]Director, Office of Hydrology, National Weather Service, 1325 East-West Hwy., Silver Spring, MD 20910

one-dimensional unsteady flow (Saint-Venant) equations. FLDWAV combines the capabilities of the popular NWS DAMBRK and DWOPER models (Fread,1993) and provides some additional features. A recent enhancement of the FLDWAV model is a new mud/debris flow routing technique in which the mud/debris flow friction slope is derived from the shear stress power-law equation of a non-Newtonian fluid. Also, a new wave-front tracking scheme is developed for modeling the mud/debris flow situations where a steep-fronted leading edge of the mud/debris wave propagates along an initially dry channel (zero initial flow), and the downstream boundary of the unsteady mud/debris flow is the wave front. In this paper, the new mud/debris flow and wave-front tracking technique is presented and its performance is tested in modeling three real mud/debris flow case studies. It is also compared with two existing expressions for the mud/debris flow friction slope term for three case studies and with some sensitivity studies.

EQUATIONS AND MODEL FORMULATION

The one-dimensional Saint-Venant unsteady flow equations used in FLDWAV as modified to include the mud/debris flow friction slope term, S_i, are (Fread, 1988, Fread 1993):

$$\frac{\partial Q}{\partial x}+\frac{\partial (A+A_0)}{\partial t}-q=0 \tag{1}$$

$$\frac{\partial Q}{\partial t}+\frac{\partial (\beta Q^2/A)}{\partial x}+gA\left(\frac{\partial h}{\partial x}+S_f+S_e+S_i\right)+L+W_f B=0 \tag{2}$$

in which t is time, x is distance along the longitudinal axis of the waterway, h is the water surface elevation, A is the active cross-sectional area of flow, A_0 is the inactive (off-channel storage) cross-sectional area of flow, q is the lateral inflow or outflow, β is the coefficient for nonuniform velocity distribution within the cross section, g is the gravity constant, S_f is the friction slope due to turbulent boundary shear stress and determined by Manning's equation, S_e is the slope due to local expansion-contraction (large eddy loss), S_i is the friction slope associated with internal viscous dissipation of non-Newtonian mud/debris fluids, L is the momentum effect of lateral flow, W_f is the wind term, and B is the channel flow width.

The additional friction slope term, S_i, in Eq.(2) is obtained by applying the rheological power-law equation of non-Newtonian fluids to a two-dimensional steady uniform open channel flow of depth, y, as follows:

$$\tau=\rho g S_i(y-z)=\tau_y+\mu\left(\frac{du}{dz}\right)^{\eta} \tag{3}$$

in which τ is the internal shear stress, u=u(z) is the longitudinal velocity in the x

direction, η is an exponent of the power-law component of the shear stress, τ_y is the yield shear strength and μ is the apparent viscosity, ρ is the bulk density of the fluid mixture, S_i is the friction slope, and $S_i = S_0$ in which S_0 is the channel bottom slope. Equation (3) can be solved for the depth mean velocity $V=f(y,\tau_y, \mu, \eta, S_i)$ by integrating over flow depth y and assuming a parabolic velocity distribution in combination with a uniform velocity for $y \geq z \geq y-\tau_y/(\gamma S_i)$ (Chen, 1983); however, the resulting equation for V is so complicated that the friction slope, S_i, cannot be derived explicitly and therefore this approach does not lend itself for unsteady flow routing purposes. Instead, an alternative semi-empirical equation which produces an approximate solution to Eq.(3) is proposed:

$$V=\frac{(0.74+0.656m)}{(m+1)(m+2)}\left(\frac{\tau_y}{\mu}\right)^m D\left(\frac{D}{D_0}-1\right)^{m+0.15} \tag{4}$$

in which $m=1/\eta$ and $m=1$ represents a Bingham fluid, D is the hydraulic depth, and $D_0=\tau_y/(\gamma S_i)$ can be regarded as the minimum depth for the mud/debris mixture to move because of the yield shear strength. The difference of the velocity profiles from Eq.(4) and that from Chen's equation is less than 5%, but an equation for S_i can be derived from Eq.(4). The derived equation for S_i can be written as:

$$S_i=\frac{\tau_y}{\gamma D}\left[1+\left(\frac{(m+1)(m+2)Q}{(0.74+0.656m)(\tau_y/\mu)^m DA}\right)^{\frac{1}{m+0.15}}\right] \tag{5}$$

In this study, the following two equations for S_i are also tested and compared with Eq. (5): (1) the equation used in NWS DAMBRK model which comes from a similar derivation from Eq.(3) in which a parabolic velocity distribution is assumed (Fread 1988); and (2) the equation based on a linear velocity distribution of laminar Bingham fluids (Jeyapalan, Duncan and Seed, 1983; Schamber and McArthur, 1985). These equations are expressed, respectively, as:

$$S_i=\frac{\tau_y}{\gamma D}\left[\frac{(m+2)}{2}+\frac{(m+2)Q}{(\tau_y/\mu)^m DA}\right]^{\frac{1}{m}} \tag{6}$$

$$S_i=\frac{\tau_y}{\gamma D}\left[1+\frac{2Q}{(\tau_y/\mu)DA}\right] \tag{7}$$

Equation (6) is equivalent to an equation used by O'Brien and Julien (1985) for a Bingham fluid (m=1). It was slightly modified in a later application (O'Brien, Julien, and Fullerton, 1993).

WAVE-FRONT TRACKING TECHNIQUE

Equations (1) and (2), together with one of the equations for S_i (Eq.(5), (6), or (7)), are solved numerically with appropriate external (upstream/downstream) and internal (dam/bridge) boundary conditions. One method in routing unsteady mud/

debris flows is to simulate them from an assumed initial mud/debris flow condition throughout the entire routing reach. There are many cases, however, where the mud/debris mixture moves over an initially very small water flow or a dry channel and often has a steep-fronted leading edge associated with the mud/debris flood wave. FLDWAV contains a new wave-front tracking technique in which the model tracks the moving wave front as its computational downstream boundary and uses an automatically generated $Q=f(y)$ loop rating as the boundary condition. Moving of the downstream boundary is controlled by checking, at every time step, the mud/debris flow volume passed from the current boundary $x=x_j$ with the minimum volume for a front-edged wave between x_j and x_{j+1} to move. Extensive tests show that this technique is excellent in simulating the moving steep-fronted waves of mud/debris flow from a zero (dry bed) or a very small initial flow condition.

APPLICATION CASE STUDIES

Case 1. Anhui Debris Dam Failure Flood

A tailings dam of the Jinshan debris reservoir in Anhui, China, breached in the early morning of April 30, 1986 (Han and Wang, 1996). The dam-break induced mud/debris flooding engulfed a village about 0.75 km downstream of the reservoir, and all of the village residents were killed in the disaster. Measurements of the inundation area were made after the flooding event.

Han and Wang simulated the unsteady mud/debris flow using a two-dimensional, depth-averaged model and assumed an inflow hydrograph as the upstream boundary condition. Data provided by these authors was used in the one-dimensional FLDWAV model to simulate the outflow from the breached dam. The following data were used: total volume of water-debris mixture in the reservoir is about 8.45×10^5 m^3; top width of the reservoir at dam is 245 m and height of the dam is 21.7 m; and the dam-break induced flow lasted less than 5 minutes. A reservoir with a final rectangular-shape dam breach of width of 240m and a 1 minute time for breach failure is modeled in the FLDWAV model. It is assumed that cross-sections are irregular trapezoids with an average width of 210m to 580m and a channel bottom slope from about 0.012 upstream to 0.00076 downstream. Values of 0.035 and 0.04 are used for Manning's n. The following Bingham fluid properties are used: $\mu=2.1$N·s/m^2 (0.044 lb·s/ft^2), $\tau_y=38$ N/m^2 (0.80 lb/ft^2), and $\gamma=15700$ N/m^3 (100 lb/ft^3). Since the initial flow is almost zero, the new wave-front tracking option is selected for the routing, and Eq.(5) is used to determine the friction slope associated with the internal viscous dissipation of the mud/debris flow.

Figure 1 shows computed mud/debris surface profiles at t=0.005, 0.01, 0.02, 0.05 and 0.09 hours. The dam breaching started at t=0.0 due to an assumed overtopping failure, and the mud/debris mixture wave front propagated downstream to a final inundation limit within a total time of about 5 minutes. This agreed with the site report that the flooding lasted less than 5 minutes. The computed flooding distance of 1200m compares well with the observed inundation distance of about

1210m. Figure 2 shows the computed discharge hydrographs at three locations along the reach (x=0 at dam site, x=400m, and x=800m). One characteristic feature simulated by the model is that the mud/debris flood wave moves with a steep front and both the discharge and stage hydrographs reach their peak very quickly. This, along with the greater density of mud/debris floods, contributes to the fact that even a small debris flood can cause devastating damage in life and property.

Figure 3 compares the computed peak discharge profiles using the different equations for S_i (Eqs.5-7) to determine the additional friction slope. In this case using these different equations produces only small computational differences.

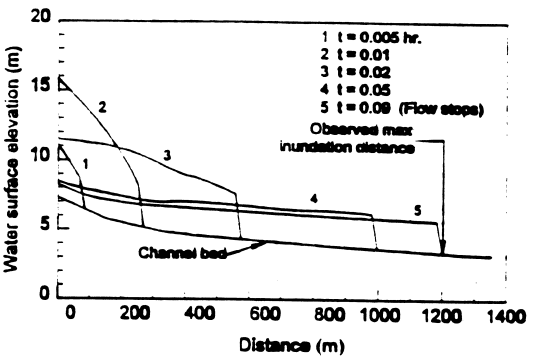

Figure 1 Computed water surface profiles for Anhui dam

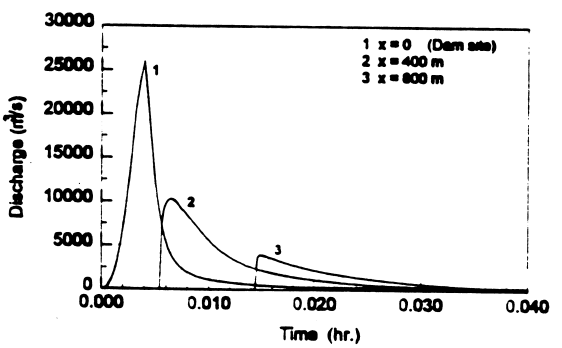

Figure 2 Computed hydrographs for Anhui dam

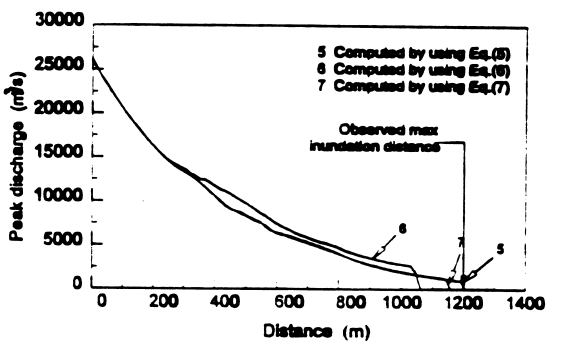

Figure 3 Peak discharge profiles for Anhui dam

Case 2. Aberfan Coal Waste Dump Failure

The Aberfan mud/debris flow disaster occurred in Wales in 1965 and was investigated by using an analytical mudflow simulation method based on the laminar Bingham fluid model (Eq.(7)) (Jeyapahan et al., 1983). In this case, waste material from a 37 m high dump from a coal-mining operation liquefied and flowed down a slope of about 12° (S_0=0.208) over a distance of about 600 m until it inundated a school and other buildings located in the flow path. One hundred and twenty lives were lost in the buried portion of the school building. The FLDWAV model is applied to this event by simulating it as a dam-break mud/debris flow case. The downstream channel has triangular cross sections with a side slope of about 1 vertical to 2 horizontal, and Manning's n of 0.05 is used in the computation. A waste reservoir is placed upstream, and the dam is breached at the

beginning of routing. The final breach has the same shape as the triangular channel cross-sections and a time of failure of about 1 minute is used to simulate the dam-failure hydrograph. The mud/debris mixture properties used are: μ=958 N·s/m^2 (20 lb·s/ft^2), τ_y=4794 N/m^2 (102 lb/ft^2), γ=17640 N/m^3 (112 lb/ft^3). Initial flow is zero and the new wave-front tracking option is used.

Figure 4 shows the computed wave-front travel times of the mud/debris flood. These results are obtained by using the three different equations for S_i. An observed data point is also shown in the figure. The results from using Eqs. (5) and (6) agree closely with the observed data, and the results from using Eq.(7) are only slightly different. The computed maximum flow depth profiles are shown in Fig.5. A small difference is noticed between using Eq.(5) and Eq.(6), while a larger difference is noted in the use of Eq.(7). Figure 6 shows computed discharge hydrographs at three locations using Eq.(5).

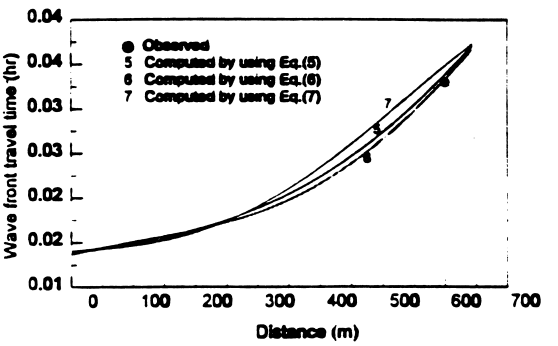

Figure 4 Wave travel times for Aberfan

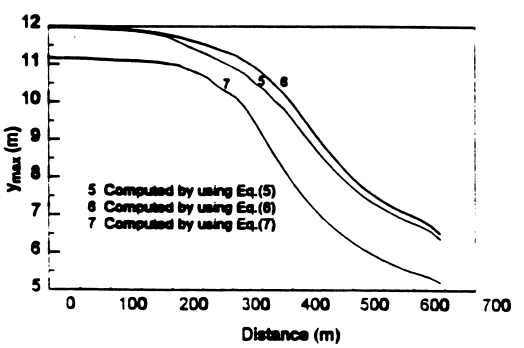

Figure 5 Peak flow depth (y_{max}) for Aberfan

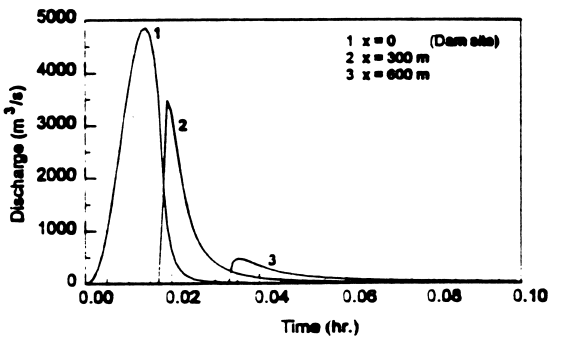

Figure 6 Computed discharge hydrogphs for Aberfan

Case 3. Rudd Creek Landslide-Induced Mudflow

The FLDWAV model is also applied to a 1983 landslide-induced Rudd Creek mud/debris flow case which occurred in Davis County, Utah. This case has been successfully simulated by using a two-dimensional unsteady mud/debris flow model (O'Brien, Julien, and Fullerton, 1993). This landslide-induced mud/debris flow submerged a residential block just downstream of the landslide. In this case, the mud/debris mixture flowed along the hill slope and not in single channel. Although the phenomena is two-dimensional, it is found that the one-dimensional model can also be used successfully. Figure 7 shows a topological map of the site. The landslide occurred at an elevation of about 4500ft (1372m). The possible flow paths are drawn in the figure. A nonprismatic channel with specifiled rectangular

cross-sections is set up. The width of the cross-sections are estimated as the distance between the possible flow paths and a reasonable extension beyond the paths according to anticipated flow depth, and the channel bottom slope can be determined according to an average elevation of the cross-sections.

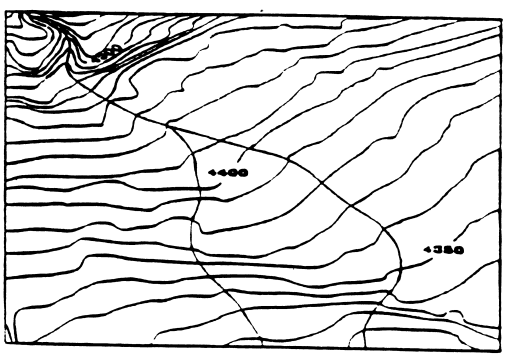

Figure 7 Top map of Rudd Creek

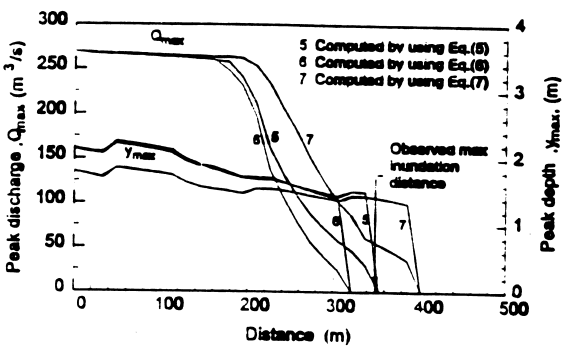

Figure 8 Computed peak flow profiles for Rudd Creek

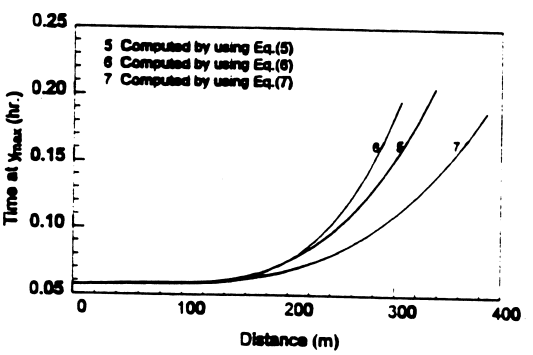

Figure 9 Wave travel times for Rudd Creek

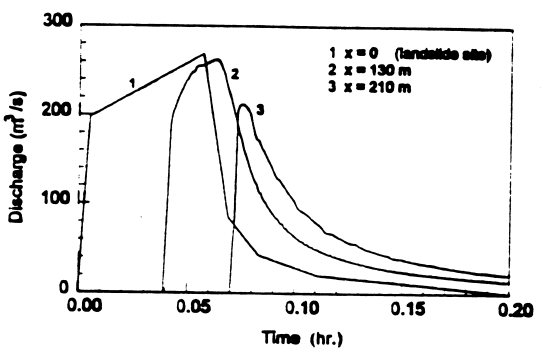

Figure 10 Computed discharge hydrographs for Rudd Creek

The debris properties are determined according to the an average of about 48% by volume mud/debris sediment concentration and an empirical relationship from experimental data (O'Brien and Julien, 1985). The following properties are used in the computations: μ=958 N·s/m^2 (20 lb·s/ft^2), τ_y=956 N/m^2 (20 lb/ft^2), and γ=15750 N/m^3 (100 lb/ft^3). The flood hydrograph used as the upstream boundary condition is shown in Fig.10 (x=0). Initial flow is zero and the wave-front tracking option is used. The computed peak discharge and mud/debris depth profiles from the three expressions for S_i are shown in Figure 8. The results of using Eq.(5) compares very well with the observed maximum inundation distance, while using Eq.(6) produced a shorter inundation distance and using Eq.(7) produced a longer distance. Figure 9 shows the computed times of maximum flow depth from which the mud/debris flow wave speed can be determined. The average wave speeds between x=100m and x=300m are 0.93 m/s (using Eq.(5)), 0.67 m/s (using Eq.(6)) and 1.67 m/s (using Eq.(7)). Eyewitness accounts estimated the wave speed from 0.6 to 1.2 m/s. Figure 10 shows the upstream hydrograph and computed hydrographs at two other locations using Eq.(5).

SENSITIVITY STUDIES

The case studies have shown that among the three equations, Eq.(5),(6) and (7), Eq.(5) provides the best performance in modeling these mud/debris flows. Some numerical experiments were also conducted to further investigate the differences in computational results by using the three equations for a range of channel slopes and mud/debris flow properties.

A mud/debris flood wave with a peak discharge of 1415m^3/s and 0.1 hour time of rise is routed through a 3218m long prismatic channel with rectangular cross-sections of width of 60m and Maning's n of 0.05. The channel is equally divided into two reaches by two bottom slopes. The upstream reach has a slope of S(1)=0.0379 (200 ft/mile) and the slope of the downstream reach, S(2), is changed to examine the effect of the slope.

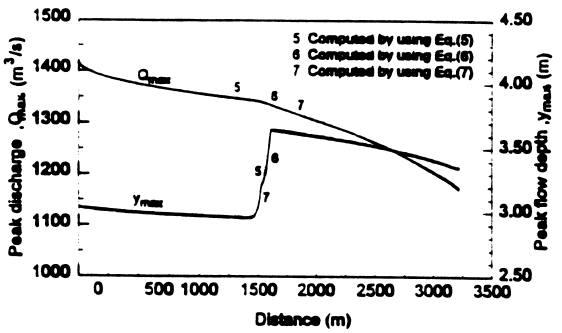

Figure 11 Test-C1

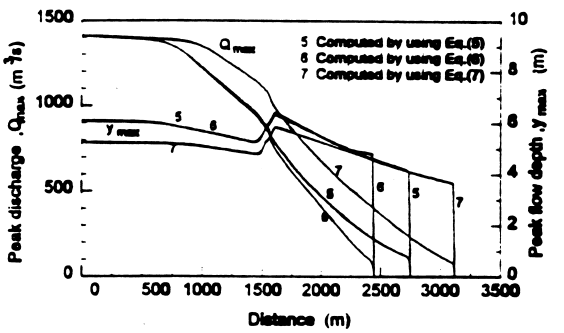

Figure 12 Test-C2

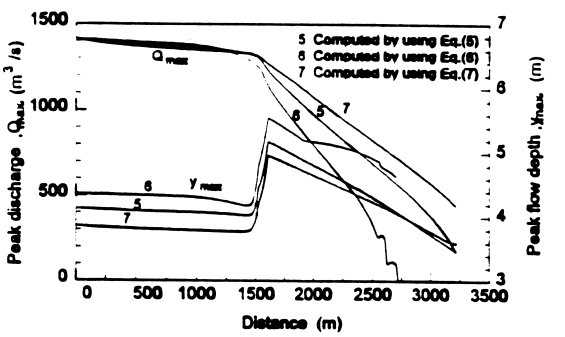

Figure 13 Test-C3

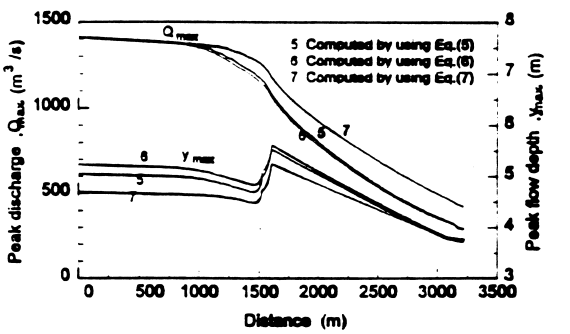

Figure 14 Test-C4

In order to evaluate the computational differences in the mud/debris flow peak profiles, the results from Eq.(5) are compared with those from Eq.(6) and from Eq.(7), and the following quantities are used to measure the differences: $\Delta Q_{5,6}$ (%) or $\Delta Q_{5,7}$ (%) is an average percentage difference in the peak discharge profile between results of Eq.(5) and Eq.(6) and between Eq.(5) and Eq.(7), $\Delta y_{5,6}$ (%) or $\Delta y_{5,7}$ (%) is an average percentage difference in the peak mud/debris flow depth profile between results of Eq.(5) and Eq.(6) and between Eq.(5) and Eq.(7). The

flow conditions and results are listed in Table 1.

Figures 11-14 show some results from one group in which S(2)=0.5×S(1) and the computed peak discharge and mud/debris flow depth profiles from the three equations are shown in the figures. It is noticed from these figures that the results from Eq.(5) are between those from Eq.(6) and those from Eq.(7). Higher values of the viscosity, μ, causes a larger departure of the results of Eq.(7) from those of Eq.(5) and Eq.(6), while higher values of the yield shear strength, τ_y, results in a larger departure of the results of Eq.(6) from those of Eq.(5) and Eq.(7).

Table 1 Mud/debris flow conditions and results

No.	S(2)	η	μ	τ_y	$\Delta Q_{5,6}$(%)	$\Delta Q_{5,7}$ (%)	$\Delta y_{5,6}$(%)	$\Delta y_{5,7}$ (%)
A-1	0.0379	1	5	5	0.001	0.01	0.02	0.10
A-2			1000	1000	3.20	21.8	0.76	7.76
A-3			100	1000	5.11	3.15	3.34	2.28
A-4			1000	100	2.00	6.87	2.80	4.40
B-1	0.0284	1	5	5	0.002	0.02	0.05	0.20
B-2			1000	1000	3.83	22.40	0.70	7.49
B-3			100	1000	6.42	3.95	4.07	5.11
B-4			1000	100	1.88	7.23	2.58	4.58
C-1	0.0190	1	5	5	0.003	0.02	0.08	0.30
C-2			1000	1000	3.33	13.20	0.55	7.07
C-3			100	1000	8.97	4.67	7.27	4.72
C-4			1000	100	1.70	7.81	2.15	4.69
D-1	0.0095	1	5	5	0.004	0.11	0.03	0.50
D-2			1000	1000	4.50	14.93	7.28	7.96
D-3			100	1000	12.00	6.38	15.00	7.12
D-4			1000	100	1.40	8.36	1.64	4.62
E-1	0.0190	2	5	5	0.10		1.83	
E-2			1000	1000	12.50		20.50	
E-3			100	1000	1.50		28.89	
E-4			1000	100	6.32		11.05	
F-1	0.0190	3	5	5	0.36		9.02	
F-2			1000	1000	26.07		29.30	
F-3			100	1000	14.41		32.98	
F-4			1000	100	13.02		17.68	

Note: S(1)=0.0379, γ=15700 N/m^3, μ=N·s/m^2, τ_y=N/m^2

These results indicate that the overall difference between Eq.(5) and Eq.(6) or between Eq.(5) and Eq.(7) are less than 15% in most situations. The largest difference between Eq.(5) and Eq.(7) occurs under the conditions where both μ

and τ_y are large values, while the largest difference between Eq.(5) and Eq.(7) occurs when the value of τ_y is large. The results in groups E and F show that the difference of Eq.(5) and Eq.(6) increases as the fluid departs from a Bingham fluid ($\eta=1$) and becomes viscoplastic ($\eta>1$). In the FLDWAV model, η can be specified as any value.

CONCLUSIONS

The one-dimensional Saint-Venant unsteady flow equations can be applied to simulate non-Newtonian mud/debris flows if an additional friction slope (S_f) representing the internal viscous dissipation is appropriately specified. The excellent computational results in the case studies show that the mud/debris flow enhanced FLDWAV model which uses Eq.(5) and a wave-front tracking technique can be a useful tool in unsteady mud/debris flow analysis associated with landslide-induced or dam-break induced mud/debris flood prediction. The sensitivity studies suggest that use of Eq.(5) in determining the mud/debris flow friction slope produces computational flow peak profiles which are between those from Eq.(6) and those from Eq.(7). The difference between Eq.(5) and Eq.(6) or between Eq.(5) and Eq.(7) are less than 15% for Bingham fluids but can be 20-30% for viscoplastic mud/debris flows.

APPENDIX I. REFERENCES

Chen, C.L. (1983). "On frontier between rheology and mudflow mechanics." in *Frontiers in hydraulic engineering* , Edited by Shen, H.T., ASCE, New York, 113-118.

Fread, D.L. (1993). Chpt 10: Flow routing, in *Handbook of Hydrology* , Edited by Maidment,D.R., McGraw-Hill, New York, 10.1-10.36

Fread, D.L. (1988). The NWS DAMBRK model: Theoretical background and user documentation, HRL-258, Hydrological Research Laboratory, National Weather Service, Silver Spring, Maryland 20910.

Han,G., and Wang,D. (1996). "Numerical modeling of Anhui debris flow." *J. Hydraulic Eng.*, ASCE, 122(5), 262-265.

Jeyapalan, J.K., Duncan, J.M., and Seed, H.B. (1983). "Analysis of flow failures of mine tailing dams." *J. Geotechnical Eng.*, ASCE, 109(2), 150-189.

O'Brien, J.S., Julien, P.Y., and Fullerton, W.T. (1993). "Two-dimensional water flood and mudflow simulation." *J. Hydraulic Eng.*, ASCE, 119(2), 244-261.

O'Brien, J.S., and Julien, P.Y. (1985). "Physical properties and mechanics of hyperconcentrated sediment flows." in *Delineation of landslide, flash flood and debris flow hazards in Utah* , UWRL/G-85/03, Utah Water Research Laboratory, Utah State University, 260-278.

Schamber, D.R., and MacArthur, R.C. (1985). "One-dimensional model for mud flows." in *Hydraulics and Hydrology in the Small Computer Age*, Vol.1, ASCE, 1334-1339..